# Multicarrier Equalization: Unification and Evaluation. Part II: Implementation Issues and Performance Comparisons. [1]

R. K. Martin, K. Vanbleu, M. Ding, G. Ysebaert, M. Milosevic, B. L. Evans, M. Moonen, C. R. Johnson, Jr. [2] [3] [4]

December 2003
Submitted for publication in IEEE Transactions on Signal Processing.

[1]This report is available by anonymous ftp from *ftp.esat.kuleuven.ac.be* in the directory *pub/sista/vanbleu/reports/03-52.pdf* and *pub/sista/ysebaert/reports/03-52.pdf*

[2]R. K. Martin and C. R. Johnson, Jr., are with the School of Electrical and Computer Engineering, Cornell University, Ithaca, NY, 14853-3801, USA (email: {frodo,johnson}@ece.cornell.edu). They were supported in part by NSF grant CCR-0310023, Applied Signal Technology (Sunnyvale, CA), Texas Instruments (Dallas, TX), and the Olin Fellowship from Cornell University.

[3]K. Vanbleu, G. Ysebaert and M. Moonen are with the Katholieke Universiteit Leuven ESAT-SCD/SISTA, 3001 Leuven Heverlee, Belgium (email: {vanbleu,ysebaert,moonen}@esat.kuleuven.ac.be). G. Ysebaert and K. Vanbleu are Research Assistants with the I.W.T. and F.W.O. Vlaanderen respectively. Their research work was carried out in the frame of (1) the Belgian State, Prime Minister s Office Federal Office for Scientific, Technical and Cultural Affairs Interuniversity Poles of Attraction Programme (2002 2007) IUAP P5/22 and P5/11, (2) the Concerted Research Action GOA-MEFISTO-666 of the Flemish Government, and (3) Research Project FWO nr. G.0196.02. The scientific responsibility is assumed by the authors.

[4]M. Ding and B. L. Evans are with the Dept. of Electrical and Computer Engineering, The University of Texas at Austin, Austin, TX 78712-1084, USA (email: {ming,bevans}@ece.utexas.edu). They were supported in part by The State of Texas Advanced Technology Program under project 003658-0614-2001. M. Milosevic was with the Dept. of Electrical and Computer Engineering at The University of Texas at Austin. He is currently with Schlumberger in Sugar Land, TX (email: milos@ece.utexas.edu).

# Multicarrier Equalization: Unification and Evaluation. Part II: Implementation Issues and Performance Comparisons

Richard K. Martin*, *Student Member, IEEE,* Koen Vanbleu, *Student Member, IEEE,* Ming Ding, *Student Member, IEEE,* Geert Ysebaert, *Student Member, IEEE,* Milos Milosevic, *Member, IEEE,* Brian L. Evans, *Senior Member, IEEE,* Marc Moonen, *Member, IEEE,* C. Richard Johnson, Jr., *Fellow, IEEE*

**Abstract**

Equalization is crucial in mitigating inter-carrier and inter-symbol interference in a multicarrier system. To ease equalization, typically a cyclic prefix (CP) is inserted between successive symbols. When the channel order exceeds the CP length, equalization can be accomplished by placing a time-domain equalizer (TEQ), in the form of a finite impulse response (FIR) filter, in cascade with the channel. The TEQ is designed to produce a shortened effective impulse response. Alternatively, a bank of equalizers can be used to remove the interference tone-by-tone. A literature survey and a unified treatment of optimal equalizer designs for multicarrier receivers were presented in Part I of this paper. This Part II focuses on implementation and performance issues. Complexity reduction techniques are discussed, and the computational complexity of these techniques is tabulated. In addition, 16 different equalizer structures and design procedures are compared in terms of achievable bit rate using synthetic and measured data.

**Index Terms:** Multicarrier, Channel Shortening, Time-domain Equalization, Complexity.

**EDICS Designation: 3-TDSL, Telephone Networks and Digital Subscriber Loops**

R. K. Martin and C. R. Johnson, Jr., are with the School of Electrical and Computer Engineering, Cornell University, Ithaca, NY, 14853-3801, USA (email: {frodo,johnson}@ece.cornell.edu). They were supported in part by NSF grant CCR-0310023, Applied Signal Technology (Sunnyvale, CA), Texas Instruments (Dallas, TX), and the Olin Fellowship from Cornell University.

K. Vanbleu, G. Ysebaert and M. Moonen are with the Katholieke Universiteit Leuven – ESAT-SCD/SISTA, 3001 Leuven–Heverlee, Belgium (email: {vanbleu,ysebaert,moonen}@esat.kuleuven.ac.be). G. Ysebaert and K. Vanbleu are Research Assistants with the I.W.T. and F.W.O. Vlaanderen respectively. Their research work was carried out in the frame of (1) the Belgian State, Prime Minister's Office – Federal Office for Scientific, Technical and Cultural Affairs – Interuniversity Poles of Attraction Programme (2002–2007) – IUAP P5/22 and P5/11, (2) the Concerted Research Action GOA-MEFISTO-666 of the Flemish Government, and (3) Research Project FWO nr. G.0196.02. The scientific responsibility is assumed by the authors.

M. Ding and B. L. Evans are with the Dept. of Electrical and Computer Engineering, The University of Texas at Austin, Austin, TX 78712-1084, USA (email: {ming,bevans}@ece.utexas.edu). They were supported in part by The State of Texas Advanced Technology Program under project 003658-0614-2001. M. Milosevic was with the Dept. of Electrical and Computer Engineering at The University of Texas at Austin. He is currently with Schlumberger in Sugar Land, TX (email: milos@ece.utexas.edu).

***Correspondence:** Richard K. Martin, 397 Frank Rhodes Hall, Cornell University, Ithaca, NY, 14853-3801 USA, Phone: (607) 254-8819, FAX: (607) 255-9072, *frodo@ece.cornell.edu*

# Multicarrier Equalization: Unification and Evaluation. Part II: Implementation Issues and Performance Comparisons

## I. Introduction

Multicarrier (MC) modulation is currently enjoying a boom in popularity, largely due to the fact that it allows an efficient receiver implementation that achieves high throughput. Discrete multitone (DMT) has been implemented in wireline MC applications such as various digital subscriber line (DSL) standards [1] and in power line communications standards. Orthogonal frequency division multiplexing (OFDM) has been implemented in wireless MC applications such as IEEE 802.11a [2] and HIPERLAN2 [3] local area networks, digital video and audio broadcast (DVB/DAB) [4], [5], and satellite radio.

One of the main advantages of MC modulation (relative to single carrier modulation) is the ease with which equalization can be performed. If the channel delay spread is shorter than the guard interval between the transmitted blocks, then the frequency-selective channel appears as a bank of adjacent flat fading channels, and equalization can be performed by a bank of scalars. If the channel delay spread is longer than this guard interval, a prefilter is needed at the receiver to shorten the effective channel to the appropriate length. This prefilter is called a time-domain equalizer (TEQ). A review of optimal TEQ designs is given in Part I of this paper [6].

An alternative to the TEQ structure is to use a bank of filters or linear combiners, one per tone, to remove the intersymbol and intercarrier interference (ISI, ICI) caused by a long channel. The filters can be placed in the time or frequency domain, leading to the TEQ filter bank (TEQFB) [7] and the Per-Tone Equalizer (PTEQ) [8], respectively.

Many equalizer designs are computationally intensive, requiring multiple matrix inversions, eigendecompositions, and Cholesky decompositions. However, the matrices involved in most designs have such a high amount of structure that many computations can be reused. Moreover, it is sometimes possible to transform the problem into a mathematically equivalent problem that requires fewer computations. The goals of this paper are:

i) to survey the complexity reduction techniques in the multicarrier equalization literature,
ii) to compare the computational cost of these methods, and
iii) to compare the bit rates of these methods for synthetic and measured ADSL channels.

The performance will be assessed in an identical manner for all designs.

Part I [6] of this paper showed that almost all TEQ designs take the form of maximizing a product of generalized Rayleigh quotients. This Part II is organized in a manner parallel to Part I. General complexity reduction techniques and fixed-point implementation issues are described in Section II. Techniques for single Rayleigh quotient designs are discussed in Sections III and IV, with a single filter or multiple filters, respectively. Techniques for designs that maximize a product of Rayleigh quotients are discussed in Section V. Section VI provides a performance comparison, and Section VII concludes the paper. The notation of Part I [6] will be retained:

- $N$ is the (I)DFT size, $\nu$ is the prefix length, $s = N + \nu$ is the symbol size, $N_u$ is the number of used tones, $\mathcal{S}$ is the set of used tones, $N_z$ is the number of unused ("null") tones, $i$ is the tone index, $k$ is the DMT symbol index, $n$ is the sample index, $\Delta$ is the synchronization delay, and $N_\Delta$ is the number of values of $\Delta$ that are considered in a given TEQ design.
- $\mathcal{F}_N$ and $\mathcal{I}_N$ are the $N$-point DFT and IDFT matrices, respectively; $\mathbf{f}_i$ is the $i^{th}$ DFT row.
- The transmitted (QAM) frequency domain symbol vector at time $k$ is $X^k$; its $i^{th}$ entry is $X_i^k$; vectors $\mathbf{x}^k$, $\mathbf{y}^k$, $\mathbf{n}^k$, and $\mathbf{u}^k$ contain the transmitted time domain samples, received samples (before the TEQ), additive noise samples, and TEQ output samples, respectively.
- The vectors $\mathbf{w}$, $\mathbf{h}$, and $\mathbf{c} = \mathbf{h} \star \mathbf{w}$ contain the TEQ, channel, and effective channel impulse responses of orders $L_w$, $L_h$, and $L_c$, respectively, where $\star$ denotes linear convolution.
- $\mathbf{0}_{m \times n}$ is the all zero matrix of size $m \times n$; $\mathbf{I}_n$ is the identity matrix of size $n \times n$.
- $(\cdot)^T$, $(\cdot)^H$, and $(\cdot)^*$ denote transpose, Hermitian, and complex conjugate respectively.
- $\mathcal{E}\{\cdot\}$ denotes statistical expectation.

## II. Complexity reduction techniques and fixed-point issues

Part I of this survey paper [6] showed that almost all TEQ designs can be classified as maximizing a cost function in the form of a product of generalized Rayleigh quotients,

$$\boxed{\hat{\mathbf{w}}^{opt} = \arg\max_{\hat{\mathbf{w}}} \prod_{j=1}^{M} \frac{\hat{\mathbf{w}}^T \mathbf{B}_j \hat{\mathbf{w}}}{\hat{\mathbf{w}}^T \mathbf{A}_j \hat{\mathbf{w}}}} \tag{1}$$

(or minimization of its inverse), where $\hat{\mathbf{w}}$ is usually the TEQ. Many TEQ designs reduce to the case of a single generalized Rayleigh Quotient ($M = 1$), which can be maximized by solving a generalized eigenvalue problem. For the more difficult case when multiple generalized Rayleigh quotients are involved ($M > 1$), numerical methods must be applied to search for the (locally) best solution. However, solutions for both the $M = 1$ and $M > 1$ cases are usually computationally expensive, and some are infeasible for a real-time implementation, especially on programmable fixed-point DSPs. Recent literature has therefore contained much work on computationally efficient methods for calculating the optimum equalizer coefficients.

### *A. Classification of complexity reduction techniques*

Some complexity reduction techniques entail no loss of optimality, whereas others use heuristics or approximations with a possible loss of optimality. We categorize the various techniques as follows:

(a) exploitation of the structure of the $\mathbf{A}_j$ and $\mathbf{B}_j$ matrices in (1), with no loss of optimality

(b) reuse of computations between different values of the synchronization delay (maintaining optimality), or reduction of the number of delays considered (possibly sub-optimal)

(c) approximation of the $\mathbf{A}_j$ and $\mathbf{B}_j$ matrices (as Toeplitz, persymmetric, or circulant, e.g.), with an expected loss of optimality

(d) use of iterative algorithms to approximate an optimal design, with an expected loss of optimality.

When $\mathbf{A}_j$ and $\mathbf{B}_j$ are structured, type (a) techniques exploit this structure when performing certain matrix operations. For instance, $\mathbf{A}_j$ and $\mathbf{B}_j$ are often constructed using correlation matrices of the transmitted and/or received signals. In [9] it was pointed out that correlation matrices are block-Toeplitz matrices and therefore some Toeplitz-based algorithms [10] could be applied to compute their inverses. Another more complicated approach is to re-use computations when computing the elements of $\mathbf{A}_j$ and $\mathbf{B}_j$ in [11] for the minimum intersymbol interference (Min-ISI) design and [12] for the maximum shortening SNR (MSSNR) design.

Most TEQ designs have $\mathbf{A}_j$ and $\mathbf{B}_j$ matrices that depend on a synchronization delay $\Delta$, which is a design parameter. Type (b) complexity reduction techniques simplify the search for the delay corresponding to optimal performance. Most designs require the solution of (1) separately for each delay, thereby making complexity proportional to the number of possible delays. If $\mathbf{A}_j(\Delta_o)$ and $\mathbf{B}_j(\Delta_o)$ depend on a delay $\Delta_o$ and only change slightly as the delay is incremented, then it may be possible to derive $\mathbf{A}_j(\Delta_o + 1)$ and $\mathbf{B}_j(\Delta_o + 1)$ from $\mathbf{A}_j(\Delta_o)$ and $\mathbf{B}_j(\Delta_o)$, rather than by recomputing the matrices entirely [12]. Another approach is to re-formulate a given design to be less delay dependent, e.g. by making either $\mathbf{A}_j$ or $\mathbf{B}_j$ independent of the delay [13], [14], and [15]. Heuristic approaches may also be adopted. Some equalizer designs (particularly those that explicitly optimize bit rate) show a performance which is smooth and optimal for a number of consecutive delays [7], [8], [16]; i.e. there exists a flat region on the bit rate performance curve. One could design the equalizer for a single delay within the expected flat region (as many vendors do), or search over a small number of possible delays [9]. The expected flat region is typically near the delay of the transmission channel itself.

Type (c) complexity reduction techniques make approximations in $\mathbf{A}_j$ or $\mathbf{B}_j$ that may induce an acceptable performance loss. One example is to approximate a Toeplitz matrix by a circulant matrix [17], [18], which has discrete Fourier transform basis vectors as eigenvectors [19]. Using the FFT and IFFT operations, the matrix computations can be carried out very efficiently.

As another example, $\mathbf{A}_j$ and $\mathbf{B}_j$ can be assumed or forced to be persymmetric [20] or Toeplitz [21], leading to a linear phase (symmetric or skew-symmetric) solution for $\hat{\mathbf{w}}$ in (1). Forcing an otherwise optimal TEQ to have linear phase leads to a substantial decrease in implementation complexity at the cost of a limited loss in bit rate [20], [21], [22], [23]. Other parameter reduction techniques (besides forcing a TEQ to have linear phase) include the reparameterization of a long FIR channel or TEQ as a pole-zero filter with fewer parameters [9], [24], and the use of the same filter (up to a scalar) for several adjacent tones in a per-tone equalizer (PTEQ) [8] or TEQ filter bank (TEQFB) [7], leading to "per group" schemes. The dual-path TEQ (DP-TEQ) structure [25] can be thought of as an extreme example of a tone-grouped TEQFB, in which one TEQ is designed for all of the tones and a second TEQ is designed to maximize bit rate on a subset of tones.

In some cases, finding the optimal solution of (1) is computationally too expensive. As a consequence, some authors resort to iterative and adaptive algorithms to obtain the solution. This is what we call a type (d) complexity reduction technique. For instance, when the equalizer design problem can be described as an eigenvalue problem, candidates to find a specific eigenvector include the generalized power method [26], gradient descent algorithms with projections [27], [28], and stochastic gradient descent algorithms with projections [29]. In addition, least-squares problems, e.g. with the PTEQ, can efficiently be solved recursively [30], [31].

Sections III, IV, and V give explicit details regarding the types (a), (b), (c), and (d) approaches described above for the cases $M = 1$ for a single filter, $M = 1$ for multiple filters, and $M > 1$ for a single filter, respectively, with $M$ as in (1).

### *B. Fixed-point implementation issues*

Any fixed-point number can be represented with $m$ bits for the integer part and $n$ bits for the fractional part. One example is the Q-format notation in Texas Instruments' C6000 DSPs. The dynamic range of the problem determines $m$ and the required precision determines $n$, although the nature of the underlying DSP induces a practical restriction on the total number of bits $(m+n)$ that can be used. Commonly, the need for the integer part is eliminated via appropriate normalization of the data, which ensures that multiplication will not change the dynamic range.

In the TEQ design problem, attention should be paid to some special matrix operations. To solve (1) with $M = 1$, which requires a generalized eigendecomposition, one standard method involves computing the Cholesky factorization of the matrix $\mathbf{B}$; see Part I [6]. However, a fixed-point implementation produces $\mathbf{A} + \Delta\mathbf{A}$ and $\mathbf{B} + \Delta\mathbf{B}$ instead of $\mathbf{A}$ and $\mathbf{B}$. The error of the computed eigenvalues is bounded by a multiple of $\kappa(\mathbf{B})\mu$, where $\kappa(\mathbf{B})$ is the condition number of $\mathbf{B}$ and $\mu$ is the unit round-off [32]. When $\mathbf{B}$ is ill-conditioned, numerical stability can be lost in the Cholesky factorization. The condition number of $\mathbf{B}$ is often large, so even with careful choices of the binary data format, the accuracy of Cholesky factorization can be unacceptable when the dimension of $\mathbf{B}$ (usually the TEQ length) is large.

The effect of round-off errors, called the digital noise floor, can be incorporated into the noise model explicity, as in [7], or implicitly, as in [16].

## III. SINGLE QUOTIENT CASES

We now consider reduced-complexity implementations of TEQ designs for the specific case of maximizing a single generalized Rayleigh quotient.

### *A. Methods for eigenvector computation*

The maximization of a single generalized Rayleigh quotient requires computation of the generalized eigenvector corresponding to the largest generalized eigenvalue of the matrix pair $(\mathbf{B}, \mathbf{A})$, as discussed in [6]. This section details general techniques for this math problem, and subsequent sections discuss details specific to particular TEQ designs.

One common iterative eigensolver is the generalized power method [10], which iterates

$$\mathbf{B}\ \hat{\mathbf{w}}_{k+1} = \mathbf{A}\ \mathbf{w}_k \tag{2}$$

$$\mathbf{w}_{k+1} = \frac{\hat{\mathbf{w}}_{k+1}}{\|\hat{\mathbf{w}}_{k+1}\|}, \tag{3}$$

which requires a square root and division at each step for the normalization, as well as an LU factorization [10] of $\mathbf{B}$ to solve (2) for $\hat{\mathbf{w}}_{k+1}$. A similar approach is to alternate between gradient descent of $\mathbf{w}^T\mathbf{A}\mathbf{w}$ and renormalization to maintain $\mathbf{w}^T\mathbf{B}\mathbf{w} = 1$:

$$\hat{\mathbf{w}}_{k+1} = \mathbf{w}_k - \mu\mathbf{A}\mathbf{w}_k \tag{4}$$

$$\mathbf{w}_{k+1} = \frac{\hat{\mathbf{w}}_{k+1}}{\|\hat{\mathbf{w}}_{k+1}\|_{\mathbf{B}}}, \tag{5}$$

where $\|\mathbf{w}\|^2_{\mathbf{B}} \stackrel{\triangle}{=} \mathbf{w}^T\mathbf{B}\mathbf{w}$ and $\mu$ is a small user-defined step size.

The expensive renormalization in (3) and (5) can be avoided through the use of a Lagrangian constraint, as in [33], [34], which leads to an iterative eigensolver of the form

$$\mathbf{w}_{k+1} = \mathbf{w}_k + \mu\left(\mathbf{B}\mathbf{w}_k - \mathbf{A}\mathbf{w}_k\left(\mathbf{w}_k^T\mathbf{B}\mathbf{w}_k\right)\right), \tag{6}$$

where $\mu$ is a small user-defined step size. If stochastic rank-one approximations of $\mathbf{B}$ and $\mathbf{A}$ are available, as in [29], then the generalized eigensolver in (6) requires $\mathcal{O}(L_w)$ multiply-adds per update. If the matrices $\mathbf{A}$ and $\mathbf{B}$ are used explicitly, (6) requires $\mathcal{O}(L_w^2)$ multiply-adds per update. In either case, (6) is amenable to fixed-point calculation. For comparison, an LU factorization or a Cholesky decomposition requires $\mathcal{O}(L_w^3)$ floating point operations, including many divisions.

### *B. The MMSE family*

There are several flavors of MMSE TEQ designs, which are distinguished based on the constraint used to avoid the trivial solution $\mathbf{b} = \mathbf{w} = \mathbf{0}$. See Part I [6] for details on the different constraints. For any MMSE method, the correlation matrices $\mathbf{R}_{xx}$, $\mathbf{R}_{xx}^{-1}$, $\mathbf{R}_{xy}$, $\mathbf{R}_{yx}$, $\mathbf{R}_{yy}$, and $\mathbf{R}_{yy}^{-1}$ must be computed. We now explain how to efficiently compute these matrices.

Typically, $\mathbf{R}_{xx}$ is delay invariant and can be approximated as a diagonal matrix, trivializing the computation of $\mathbf{R}_{xx}^{-1}$. In downstream ADSL, e.g., tones 33–256 are used, which makes $\mathbf{R}_{xx}$ almost the identity. The channel output autocorrelation $\mathbf{R}_{yy}$ is also delay invariant, Toeplitz, and symmetric, but not diagonal. Computing the inverse of such a matrix, i.e. $\mathbf{R}_{yy}^{-1}$, requires only $\mathcal{O}\left(3L_w^2\right)$ instead of $\mathcal{O}\left(L_w^3\right)$ operations [10, Section 4.7.4]. Moreover, when $\mathbf{R}_{yy}^{-1}$ is approximated by a circulant matrix, its inverse can be performed by means of DFTs [17], [18].

If the channel is known explicitly, then the matrices $\mathbf{R}_{xy}$, $\mathbf{R}_{yx}$ and $\mathbf{R}_{yy}$ can be written in terms of the channel coefficients, as in [35]. Otherwise, computation of $\mathbf{R}_{xy}$ and $\mathbf{R}_{yx}$ can be simplified by re-using computations from one delay $\Delta$ to the next. Note that

$$[\mathbf{R}_{yx}(\Delta+1)]_{(0:L_w,0:\nu-1)} = [\mathbf{R}_{yx}(\Delta)]_{(0:L_w,1:\nu)}\,, \tag{7}$$

which provides the bulk of $\mathbf{R}_{yx}(\Delta+1)$ for free. Moreover, the matrix [35], [36], [37]

$$\mathbf{R}(\Delta) = \mathbf{R}_x - \mathbf{R}_{xy}\mathbf{R}_y^{-1}\mathbf{R}_{yx}, \tag{8}$$

is used for a unit norm constraint on $\mathbf{b}$, for example. This matrix must also be computed for every delay. Using (7), we have [12]

$$[\mathbf{R}(\Delta+1)]_{(0:\nu-1,0:\nu-1)} = [\mathbf{R}(\Delta)]_{(1:\nu,1:\nu)}\,. \tag{9}$$

In fact, (9) holds for all MMSE designs, not just for the unit norm constraint on $\mathbf{b}$. For each new delay, only the last column of $\mathbf{R}(\Delta+1)$ must be computed, and the last row is obtained by symmetry. Moreover, the speed of the computation of the eigenvector of $\mathbf{R}(\Delta+1)$ can be increased by using a shifted version of the target impulse response (TIR) for delay $\Delta$ to initialize the eigensolver for delay $\Delta+1$ [12].

Approximations can be made to further simplify the computations. For instance, [36] first proposes the use of a representative class of channels, and then pre-computes the desired TIR for each channel. When an actual channel is measured, the TIR is selected as the one corresponding to the pre-defined channel that best matches the actual channel [36]. The TEQ is then computed to match the given channel to the precomputed TIR.

Impulse reponses can also be approximated as symmetric. For an infinite length TEQ, the finite length MMSE TIR will be symmetric or skew-symmetric [21]. Thus, it is reasonable to enforce a finite-length symmetric TIR. This reduces the complexity of the eigensolver by a factor of 4, at a loss of about 10% of the bit rate for a 20-tap TEQ [12].

An alternate approach is to avoid the matrix computation and eigenvector solver altogether via an iterative algorithm. The MMSE design was originally proposed in a form similar to (4) and (5), except with simultaneous gradient descent on both the TIR and the TEQ [35]. However, this approach is often slow to converge [1], [38]. Moreover, this adaptive algorithm requires time-domain training, which is only available if there is training on all of the frequency bins in a given symbol. This is not the case in many multicarrier standards, for example Digital Video Broadcast [4]; and in ADSL, the training is only available during the initial handshake period and every 69$^{th}$ symbol thereafter. This can in principle be remedied by using decision-direction if one is willing to tolerate a delay of an entire block before decisions can be made, perhaps by updating at the symbol rate rather than at the sample rate.

The computational complexity for several MMSE designs is summarized in Table I. The most efficient techniques are used in all cases, including applying (9) during matrix computations and not repeating matrix inversions at each delay unless the matrix is delay-dependent.

TABLE I

COMPLEXITY OF MMSE DESIGNS. MACS ARE REAL MULTIPLY-AND-ACCUMULATE OPERATIONS.

| Optimal design | Complexity per delay |
|---|---|
| MMSE, UTC on $\mathbf{b}$ [9] | $\mathcal{O}\left(\frac{1}{3}\nu^3 + \nu^2 + 2\nu L_w + L_w^2\right)$ MACs |
| MMSE, UTC on $\mathbf{w}$ [39] | $\mathcal{O}\left(\frac{1}{3}\nu^3 + \nu^2 + \nu L_w\right)$ MACs |
| MMSE, UNC on $\mathbf{b}$ [35] | $\mathcal{O}\left(\nu^2 + 2\nu L_w + 2L_w^2\right)$ MACs |
| MMSE, UNC on $\mathbf{w}$ [39] | $\mathcal{O}\left(\nu^2 + \nu L_w + L_w^2\right)$ MACs |
| Sym-MMSE, UNC on $\mathbf{b}$ [12] | $\mathcal{O}\left(\nu^2 + \frac{3}{2}\nu L_w + \frac{5}{4}L_w^2\right)$ MACs |
| Adaptive design | Complexity per update per delay |
| Adaptive MMSE [35] | $\mathcal{O}\left(4\nu + 2L_w\right)$ MACs + square root + division |

### C. Chow's TEQ training algorithm

In [38], Chow *et al.* describe an efficient TEQ training algorithm. It is meant as a computationally inexpensive iterative algorithm (by reusing the available hardware such as FFT/IFFT blocks) that approximates the MMSE TEQ with unit-norm constraint on $\mathbf{b}$ while avoiding expensive matrix inversions [1]. However, the algorithm does not ensure convergence to the MMSE TEQ.

Each iteration consists of 4 steps: an update of the TIR $\mathbf{b}$, a windowing of $\mathbf{b}$ to $\nu + 1$ taps, an update of the TEQ $\mathbf{w}$, and a windowing of $\mathbf{w}$ to $L_w + 1$ taps. The updates are performed in the frequency domain ($B^{win} = \mathcal{F}\{\mathbf{b}\}$, $W^{win} = \mathcal{F}\{\mathbf{w}\}$), either by an instantaneous zero forcing update or a frequency domain LMS update:

$$B_i = \frac{W_i^{\text{win}} Y_i^k}{X_i^k} \quad \text{or} \quad B_i = B_i^{\text{win}} + \mu (X_i^k)^* (W_i^{\text{win}} Y_i - B_i^{\text{win}} X_i) \quad \text{and} \tag{10}$$

$$W_i = \frac{B_i^{\text{win}} X_i^k}{Y_i^k} \quad \text{or} \quad W_i = W_i^{\text{win}} + \mu (Y_i^k)^* (B_i^{\text{win}} X_i - W_i^{\text{win}} Y_i) \tag{11}$$

The time-domain windowing is performed on the inverse FFT of $W$ and $B$ such that only the $L_w + 1$ and $\nu + 1$ samples with highest total energy are retained. An algorithm outline and the computational complexity for Chow's algorithm are given in Table II.

TABLE II

OUTLINE AND COMPLEXITY (PER ITERATION) OF CHOW'S ALGORITHM, USING DIVISION FOR $B_i$ IN (10) AND LMS FOR $W_i$ IN (11). MACS ARE REAL MULTIPLY-AND-ACCUMULATE OPERATIONS.

| Operation | Complexity per iteration |
|---|---|
| 1. update $B$ | $\mathcal{O}(4N)$ MACs & 1 FFT |
| 2. window $\mathbf{b}$ | $\mathcal{O}(2N)$ MACs & 1 FFT |
| 3. normalize $\mathbf{b}$ | 1 square root & 1 division |
| 4. update $W$ | $\mathcal{O}(4N)$ MACs & 1 FFT |
| 5. window $\mathbf{w}$ | $\mathcal{O}(2N)$ MACs & 2 FFTs |
| total: | $\mathcal{O}(N(12 + 5\log_2(N)))$ MACs + 1 square root + 1 division |

### *D. The MSSNR family*

This section discusses the MSSNR TEQ design [40] and its extensions, including symmetric and skew-symmetric MSSNR TEQs [20], [22] and related methods such as the Minimum Inter-symbol Interference (Min-ISI) method [26], the Minimum Inter-block Inferference (Min-IBI) method [33], and Minimum Delay Spread (MDS) methods [13], [14].

First, consider the standard MSSNR design. Following [40], we define $\mathbf{H}$ as the channel convolution matrix of size $(L_c + 1) \times (L_w + 1)$, $\mathbf{H}_{win}$ as rows $\Delta$ through $\Delta + \nu$ of $\mathbf{H}$ (with row indexing starting at zero), and $\mathbf{H}_{wall}$ as the remaining rows of $\mathbf{H}$. Details can be found in [6]. The MSSNR design problem can be stated as [41]

$$\max_{\mathbf{w}} \left( \mathbf{w}^T \underbrace{\mathbf{H}_{win}^T \mathbf{H}_{win}}_{\mathbf{B}} \mathbf{w} \right) \quad \text{subject to} \quad \mathbf{w}^T \underbrace{\mathbf{H}_{wall}^T \mathbf{H}_{wall}}_{\mathbf{A}} \mathbf{w} = 1. \tag{12}$$

It has been shown that maximizing the energy of the "windowed" portion of the effective channel with respect to the energy of the "walled" portion leads to the same TEQ as maximizing the energy of the "windowed" portion of the effective channel with respect to the energy of the entire channel [42]. Thus, (12) is equivalent to

$$\max_{\mathbf{w}} \left( \mathbf{w}^T \underbrace{\mathbf{H}_{win}^T \mathbf{H}_{win}}_{\mathbf{B}} \mathbf{w} \right) \quad \text{subject to} \quad \mathbf{w}^T \underbrace{\mathbf{H}^T \mathbf{H}}_{\mathbf{C}} \mathbf{w} = 1. \tag{13}$$

The solution for $\mathbf{w}$ will be the generalized eigenvector of the matrix pair $(\mathbf{B}, \mathbf{C})$ corresponding to the largest generalized eigenvalue $\lambda$; note that $\mathbf{C}$ takes on the role of $\mathbf{A}$ in (1). Since $\mathbf{C}$ is not a function of delay $\Delta$, it only needs to be computed once, and since it is symmetric and Toeplitz, it can be computed in its entirety by computing only the first column. Moreover, (12) requires a Cholesky decomposition of $\mathbf{A}$ or $\mathbf{B}$ for each $\Delta$, but since $\mathbf{C}$ is not delay dependent, only one Cholesky decomposition is needed for (13). Thus, we will refer to (13) rather than (12). A similar implementation, with a generalization to reduce noise gain, was proposed in [15].

To solve (13), the $(L_w{+}1)\times(L_w{+}1)$ matrix $\mathbf{B}$ must be computed for each of the possible values of $\Delta$, and for each $\Delta$ a generalized eigenvector must be computed. Reducing the complexity can be accomplished by reducing the computation of $\mathbf{B}$, or by reducing the computation of the eigenvectors. One way to re-use computations is to obtain all but the first row and column of $\mathbf{B}(\Delta + 1)$ by shifting in all but the last row and column of $\mathbf{B}(\Delta)$ [12],

$$[\mathbf{B}(\Delta + 1)]_{(1:L_w,1:L_w)} = [\mathbf{B}(\Delta)]_{(0:L_w-1,0:L_w-1)} \tag{14}$$

in a manner similar to (9). The first column of $\mathbf{B}(\Delta{+}1)$ can then be quickly obtained as follows. Since $\mathbf{B}$ is nearly Toeplitz, instead of computing a full $(\nu + 1)$-length dot product to get each element, only two multiply-adds are needed [11]:

$$\mathbf{B}_{(m,n)} = \mathbf{B}_{(m+1,n+1)} + h(\Delta + \nu + 1 - m)\ h(\Delta + \nu + 1 - n) - h(\Delta - m)\ h(\Delta - n). \tag{15}$$

The first row can then be obtained by transposing the first column. The $\mathbf{B}$ for the first delay considered can also be computed almost entirely via (15).

Further reductions in complexity can be obtained by reducing the number of delay values that are searched (possibly creating sub-optimal performance), or by using a shifted version of the TEQ for delay $\Delta$ to initialize the eigensolver for the TEQ for delay $\Delta + 1$ [12].

Similar complexity reduction techniques can be applied to MSSNR variants such as the Min-ISI method [26], the Min-IBI method [33], and the Minimum Delay Spread (MDS) method [13]. For example, in the Min-ISI method, the ISI is weighted in the frequency domain, leading to a more complicated $\mathbf{B}$ matrix (see [6]). The above techniques still apply, although (15) must be modifed as in [11].

The Min-IBI and MDS designs are part of a larger class defined in [15]. Consider minimizing

$$J = \alpha \frac{\sum_n f(n - n_{mid}) \left|\mathbf{c}_n\right|^2}{\sum_n \left|\mathbf{c}_n\right|^2} + (1 - \alpha) \frac{\sigma_w^2}{\sigma_x^2 \|\mathbf{c}\|^2}, \tag{16}$$

where $n_{mid}$ is the desired "middle" of the non-zero portion of the effective channel and $f(\cdot)$ is an arbitrary function. The case $\alpha = 1$ and $f(n) = n^2$ leads to an algorithm that minimizes the delay spread (MDS) of the effective channel [13]. The case $\alpha = 1$ and

$$f(n) = \begin{cases} 0, & -\frac{\nu}{2} \leq n \leq \frac{\nu}{2} \\ 1, & \text{otherwise} \end{cases} \tag{17}$$

leads to an algorithm which minimizes $\mathbf{w}^T\mathbf{A}\mathbf{w}$ while keeping $\mathbf{w}^T\mathbf{C}\mathbf{w} = 1$ [with $\mathbf{A}$ and $\mathbf{C}$ as in (12) and (13)]. For general values of $\alpha$ ("Noise-limited MSSNR," or NL-MSSNR), (15) still applies, since the noise term does not change the near-Toeplitz structure of the matrices.

Hitherto, the MSSNR complexity reduction techniques have focused on finding the same SSNR-maximizing solution at a lower cost. An alternate philosophy is to use approximations or iterative algorithms to find nearly the same solution at reduced cost. Symmetric MSSNR (Sym-MSSNR) constrains the impulse response to have linear phase (symmetric or skew-symmetric), so only half of the TEQ coefficients need to be computed. This reduces the complexity of the eigensolver by a factor of 4. However, the bit rates of the constrained MSSNR solution drop by about 3% for ADSL and VDSL systems [12], [20], [22].

One iterative method of solving (13) is the generalized power method of (2) and (3). Other iterative/adaptive MSSNR techniques have been proposed in [27] and [29]. These techniques are similar to the power method, but perform a gradient descent of a cost function (rather than a matrix multiply) with a periodic renormalization. Alternatively, (6) can be used to avoid the renormalization.

The computational complexity for MSSNR designs is summarized in Table III. The MSSNR, NL-MSSNR, and Sym-MSSNR designs assume that the methodology of (13), (14), and (15) are used. The Min-ISI design assumes that the efficient matrix computations of [11] are used, which are a generalization of (15). The method of [29] is assumed to use a stochastic update of the form of (6). The method of [27] requires a constraint to avoid $\mathbf{w} = \mathbf{0}$, which can be enforced through periodic renormalization, for example. The method of enforcing the constraint could add considerably to the algorithm's complexity. The power method assumes that the Cholesky decomposition of $\mathbf{B}$ needed to solve (2) is only performed once, rather than at each iteration.

TABLE III

COMPLEXITY OF MSSNR DESIGNS. MACS ARE REAL MULTIPLY-AND-ACCUMULATE OPERATIONS, AND FLOPS ARE REAL FLOATING POINT OPERATIONS (I.E., INCLUDING DIVISIONS).

| Optimal design | Complexity per delay |
|---|---|
| MSSNR [40] and NL-MSSNR [15] | $\mathcal{O}\left(L_w^3\right)$ flops |
| Sym-MSSNR [20] | $\mathcal{O}\left(\frac{1}{8}L_w^3\right)$ flops |
| Min-ISI [26] | $\mathcal{O}\left((5NL_w + L_w^3)\right)$ flops |
| Min-IBI [33] | $\mathcal{O}\left((L_cL_w^2 + \frac{5}{3}L_w^3)\right)$ flops |
| MDS [13] | $\mathcal{O}\left((L_cL_w^2 + L_w^3)\right)$ flops |
| **Iterative/adaptive design** | **Complexity per delay** |
| MSSNR via power method (2) [10] | $\mathcal{O}\left(3L_w^2\right)$ MACs/update |
| MSSNR via iteration of (6) [34] | $\mathcal{O}\left(2L_w^2\right)$ MACs/update |
| MERRY [29] | $\mathcal{O}\left(4L_w\right)$ MACs/update |
| Nafie & Gatherer [27] | $\mathcal{O}\left(2L_w\right)$ MACs/update + (1 square root and 1 division)/update |
| Iterative Min-ISI [23] | $\mathcal{O}\left(N^3\right)$ MACs + $\mathcal{O}\left(3L_w^2\right)$ MACs/update + (1 square root and 1 division)/update |

## *E. The CNA adaptive equalizer*

In many multicarrier standards [2], [3], [4], [5], the frequency-domain input signal is zero-padded before transmission, so some frequency bins $X_i$ are null (zero). In the absence of ISI, each corresponding receiver FFT output $U_i$ is expected to also be zero; whereas in the presence of ISI, it may not. The carrier-nulling algorithm (CNA) [43], [44] performs a stochastic gradient descent of the output energy in the set of $N_z$ null carriers, where a periodic renormalization is used to avoid $\mathbf{w} = \mathbf{0}$. This constrained minimization problem is in fact an eigenvector problem, and the CNA algorithm becomes a low-complexity adaptive eigenvector estimator which equalizes the channel to an impulse, rather than shortening it to a window [43]. The computational complexity of CNA is given in Table IV.

TABLE IV

COMPUTATIONAL COMPLEXITY OF CNA. MACS ARE REAL MULTIPLY-AND-ACCUMULATE OPERATIONS.

| Operation | Complexity per iteration |
| --- | --- |
| additive update | $\mathcal{O}\left(N\left(N_z+L_w\right)\right)$ MACs |
| renormalization | 1 square root & 1 division |

## IV. MULTIPLE FILTERS, EACH WITH A SINGLE QUOTIENT

The design methods called a per tone equalizer (PTEQ) and a time domain equalizer filter bank (TEQFB) treated in this section discontinue the practice of using only one filter to equalize the channel across the entire bandwidth, and instead assign each subchannel a potentially different equalizing filter. Both methods use the measure achievable bit rate as their objective function, thus also breaking away from the practice of earlier methods (e.g. in Sections II and III) that maximized objective functions that were not necessarily related to the bit rate of the system. Both methods were reviewed in Part I of this paper [6], focusing on the equalizer architecture and design premises. This section describes the implementation of these methods, with emphasis on the computational complexity encountered during equalizer coefficient initialization and data transmission.

### A. Per-tone equalizer

The PTEQ architecture [8] allows one equalizer in the *frequency domain* for each subchannel. PTEQ moves the equalization after the FFT block and incorporates the functions of the FEQ as well. The PTEQ derivation (reviewed in Part I) starts from the conventional single time domain architecture and uses the linearity of all operations to arrive at the frequency domain equalizer $\mathbf{w}_i$ for subchannel $i$. We can write the equalized output on tone $i$ as [30]

$$\tilde{X}_i^k = \bar{\mathbf{v}}_i^T \mathbf{F}_i \mathbf{y}^k \tag{18}$$

where $\tilde{X}_i^k$ is the estimate of the transmitted symbol $X_i^k$ in subchannel $i$, $\bar{\mathbf{v}}_i^T$ are PTEQ equalizer coefficients for tone $i$ incorporating the sliding FFT subtraction terms [8], $\mathbf{y}^k$ is a vector of $N+L_w$ samples in symbol $k$, and

$$\mathbf{F}_i = \left[\begin{array}{c|c|c} \mathbf{I}_{L_w} & \mathbf{0} & -\mathbf{I}_{L_w} \\ \hline \mathbf{0} & \multicolumn{2}{c}{\mathbf{f}_i} \end{array}\right] \tag{19}$$

Here, $\mathbf{f}_i$ performs the single-point DFT. The optimal coefficients are then arrived at by minimizing

$$J(\mathbf{v}_i) = E[|\bar{\mathbf{v}}_i^T \mathbf{F}_i \mathbf{y}^k - X_i^k|^2] \tag{20}$$

The cost function (20) can be minimized using several direct methods discussed in Part I, either with or without the knowledge of the channel state information and noise and signal statistics. Direct methods require a transmission of a training sequence of $K$ symbols and a large number of computations, although an adaptive method would have lower numerical complexity.

An adaptive PTEQ method minimizing (20) based on recursive least squares (RLS) with inverse updating is given in [30]. This RLS-based method estimates the covariance matrix of the equalizer input $\mathbf{R}_i^k = \sum_{j=1}^{k} (\mathbf{F}_i \mathbf{y}^j)^* (\mathbf{F}_i \mathbf{y}^j)^T$ and decomposes it into $(\mathbf{R}_i^k)^{-1} = (\mathbf{L}_i^k)^H \mathbf{L}_i^k$ where $\mathbf{L}_i^k$ is a lower triangular matrix. The algorithm then for $K$ iterations directly improves the estimate of $\mathbf{L}_i^k$ [without recomputing $(\mathbf{R}_i^k)^{-1}$] and uses the byproduct of that refinement in an RLS-based adaptation for the equalizer coefficients $\mathbf{v}_i^k$. The reader should see [30] for further details. Most important, the inclusion of the sliding FFT difference terms induces a special structure in $\mathbf{L}_i^k$ where the matrix $\mathbf{L}_i^k(0 : L_w - 1, 0 : L_w - 1)$ is real and equal for all subchannels and only the last row of $\mathbf{L}_i^k$ is different and complex. A combined RLS-LMS initialization technique is described in [31].

The RLS initialization complexity, assuming that all of the available subchannels are used, is $\frac{N}{2}(20L_w + 30) + 3L_w^2 + 7L_w$ MACs/iteration, while the RLS-LMS complexity under the same assumptions is $\frac{N}{2}(4L_w + 13) + 3L_w^2 + 7L_w$ MACs/iteration [31].

Note, that in contrast to direct PTEQ initialization methods, the RLS PTEQ does not need knowledge of the channel state and the noise statistics. The simulation results reported in [30] show that for the given examples, the RLS-based initialization algorithm achieves a data rate and SNR similar to the direct methods for the same number of training symbols.

### *B. Time domain equalizer filter bank*

A per tone method with a *time domain* equalizer for each subchannel is the TEQ Filter Bank (TEQFB) [7]. The method models the subchannel SNR as a single generalized Rayleigh quotient

$$\mathrm{SNR}_i = \frac{\mathbf{w}^T \tilde{\mathbf{B}}_i \mathbf{w}}{\mathbf{w}^T \tilde{\mathbf{A}}_i \mathbf{w}}, \tag{21}$$

where the complex-valued Hermitian symmetric $(L_w+1)\times(L_w+1)$ matrices are

$$\tilde{\mathbf{A}}_i = 2S_{x,i}\left(\underbrace{\mathbf{H}_{wall,1}^T\mathbf{V}_i\mathbf{V}_i^H\mathbf{H}_{wall,1}}_{\mathbf{A}_{i,h}} + \underbrace{\mathbf{H}_{wall,2}^T\mathbf{W}_i\mathbf{W}_i^H\mathbf{H}_{wall,2}}_{\mathbf{A}_{i,t}}\right) \quad (22)$$

$$+ \underbrace{\mathbf{Q}_i^{\text{noise}}\mathbf{R}_n\left[\mathbf{Q}_i^{\text{noise}}\right]^H}_{\mathbf{A}_{i,awgn}+\mathbf{A}_{i,next}+\mathbf{A}_{i,adc}} + \frac{\sigma_{\text{DNF}}^2}{\mathbf{w}^T\mathbf{w}}\mathbf{I}_{L_w+1},$$

$$\tilde{\mathbf{B}}_i = S_{x,i}\mathbf{H}^T\mathbf{Q}_i^{\text{circ}}\left[\mathbf{Q}_i^{\text{circ}}\right]^H\mathbf{H}. \quad (23)$$

$\mathbf{H}_{wall,1}$ and $\mathbf{H}_{wall,2}$ are convolution matrices composed of the head and tail portions of the channel, $\mathbf{h}(0:\Delta-1)$ and $\mathbf{h}(\Delta+\nu+1:N)$, respectively; $\mathbf{V}_i$ and $\mathbf{W}_i$ are upper and lower triangular Hankel matrices made from the $i^{\text{th}}$ row of the DFT matrix, $\mathbf{f}_i$; $\mathbf{Q}_i^{\text{noise}}$ and $\mathbf{Q}_i^{\text{circ}}$ are Hankel matrices made from $\mathbf{f}_i$ that account for the DMT symbol structure; $\mathbf{R}_n$ is the noise (AWGN, crosstalk and finite precision of analog-to-digital converter) covariance matrix; and $\sigma_{\text{DNF}}^2$ is the power of the noise due to the fixed-point arithmetic [7]. The TEQFB design involves computing $\tilde{\mathbf{A}}_i$ and $\tilde{\mathbf{B}}_i$ as in (22) and (23), then maximizing a generalized Rayleigh quotient for each subchannel. The efficient TEQFB initialization procedure in [45] exploits the structure of these matrices to reduce the number of computations necessary for their initialization compared to a straight multiply-update approach that would be taken if no such structure existed.

*1) Subchannel SNR model numerator:* Element $k,j$ of $\tilde{\mathbf{B}}_i$ can be written as

$$\tilde{\mathbf{B}}_i[k,j] = N\mathbf{f}_i[k-j]\underbrace{\left(\sum_{m=0}^{N+L_w-2-k}\mathbf{h}[m]\mathbf{f}_i[m]\right)}_{\mathbf{t}_i[k]}\underbrace{\left(\sum_{l=0}^{N+L_w-2-j}\mathbf{h}[l]\mathbf{f}_i[-l]\right)}_{\mathbf{t}_i^*[k]} \quad (24)$$

where $0\le k\le L_w$. A recursive formula for the computation of elements $\mathbf{t}_i[k]$ is given in [45]. Computation of the lower triangle elements of $\tilde{\mathbf{B}}_i$ requires order $\mathcal{O}\left(\max(L_w^2,N)\right)$ real multiply-accumulate (MAC) operations[1].

*2) Subchannel SNR model denominator:*

*a) AWGN and ADC component:* The AWGN and ADC contribution is captured in $\mathbf{A}_{i,awgn}+\mathbf{A}_{i,adc}$, which is a Hermitian symmetric and Toeplitz matrix. Thus, it is only necessary to compute elements of its first column. The remaining elements are then defined by the Hermitian symmetry and Toeplitz structure.

[1] In standardized ADSL the largest value of $N$ used is 512 and $L_w$ often ranges from 2 to 32 for customer premises equipment.

*b) Near-end crosstalk component:* The matrix $\mathbf{A}_{i,next} = \mathbf{Q}_i^{\text{noise}} \mathbf{R}_{next} \left[\mathbf{Q}_i^{\text{noise}}\right]^H$ where the noise covariance matrix $\mathbf{R}_{next}$ is symmetric and Toeplitz. Hence,

$$\mathbf{A}_{i,next}[k,j] = \sum_{n=0}^{N-1} \sum_{m=0}^{N-1} \mathbf{R}_{next}[|n-m+i-j|, 0] \mathbf{f}_i[m-n] \tag{25}$$

The dependence of the element $\mathbf{A}_{i,next}[k,j]$ on the index $i-j$ of matrix $\mathbf{R}_{next}$ means that $\mathbf{A}_{i,next}$ also is symmetric and Toeplitz and only the first column needs to be calculated. The algorithm requires $\mathcal{O}\left(4N + 15L_w\right)$ real MACs [45].

*c) Channel tail component:* Define the temporary Hankel matrix $\mathbf{X}_i = \mathbf{H}_{wall,2}^T \mathbf{W}_i$. It is shown in [45] that the element $\mathbf{A}_{i,t}^{k,j}$ is recursively defined as

$$\begin{aligned} \mathbf{A}_{i,t}[L_w-1,j] &= \sum_{g=L_w-1}^{\Delta-1} \mathbf{X}_i[0,g] \sum_{s=0}^{\Delta-L_w+j} \mathbf{X}_i^H[0,s], & (26) \\ \mathbf{A}_{i,t}[k,j] &= \mathbf{A}_{i,t}[k+1,j+1] + \mathbf{X}_i[0,k]\mathbf{X}_i^H[0,j]. & (27) \end{aligned}$$

Computation of the lower triangle elements of $\mathbf{A}_{i,t}$ requires exactly $7L_w^2 + 4L_w\Delta + 5\Delta - 3L_w$ MAC operations. Usually $\Delta > L_w$, so the described algorithm requires $\mathcal{O}\left(4L_w\Delta\right)$ MACs.

*d) Channel head component:* Define $\mathbf{Z}_i = \mathbf{H}_{wall,1}^T \mathbf{V}_i$. A recursive relationship can be defined between the elements of the $k^{\text{th}}$ row of $\mathbf{Z}_i$:

$$\mathbf{Z}_i[k,j+1] = \mathbf{f}_i[1]\mathbf{Z}_i[k,j] + \mathbf{h}[(N+L_w-2)-k-(j+1)]. \tag{28}$$

This algorithm for calculation of $\mathbf{A}_{i,h}$ will update the value of all of the matrix elements with the contribution of the product the $j^{\text{th}}$ column of $\mathbf{Z}_i$ and the $j^{\text{th}}$ row of $\mathbf{Z}_i^H$ for $0 < j < N - \nu - \Delta + L_w - 1$. The algorithm requires order $\mathcal{O}\left(NL_w^2\right)$ MACs.

The overall initialization complexity of TEQFB is of the order $\mathcal{O}\left(8L_w^2 N\right)$ per subchannel. Assuming that $N/2$ subchannels are used, that there are $N$ frames to complete initialization[2] and that the duration of a frame is $(N+\nu)/f_s$ where $f_s = 2.208$ MHz is the sampling frequency, the TEQFB initialization complexity is approximately $4L_w^2 f_s$ MACs / s.

### C. Data transmission complexity

The computational complexity and memory requirements during data transmission (as opposed to initialization) for the TEQFB and PTEQ architectures are shown in Table V. Thus, a TEQFB

[2]Assuming that the channel state and noise statistics are already known

TABLE V

DATA TRANSMISSION COMPUTATIONAL COMPLEXITY FOR SAMPLE RATE $f_\mathrm{s} = 2.208$ MHZ, SYMBOL RATE $f_\mathrm{sym} = 4$ KHZ, FFT SIZE $N = 512$, CYCLIC PREFIX LENGTH $\nu = 32$, AND ASSUMING $\frac{N}{2}$ DATA-CARRYING SUBCHANNELS.

| **PTEQ** | **MACs / s** | **Storage Words** |
|---|---|---|
| FFT | $2N \log_2 N f_\mathrm{sym}$ | $4N + 2\nu$ |
| Difference terms | $L_w f_\mathrm{sym}$ | $L_w$ |
| Combiner | $N(L_w + 2) f_\mathrm{sym}$ | $(L_w + 1)N$ |
| 8-tap example | $57 \cdot 10^6$ | 6728 |
| **TEQFB** | **MACs / s** | **Storage Words** |
| TEQ FB | $\frac{N}{2} L_w f_\mathrm{s}$ | $L_w(\frac{N}{2} + 1)$ |
| Goertzel FB | $(N^2 + N) f_\mathrm{sym}$ | $4N$ |
| FEQ | $2N f_\mathrm{sym}$ | $N$ |
| 8-tap example | $5577 \cdot 10^6$ | 4616 |

can have lower memory needs than a PTEQ; however, a TEQFB has significantly higher computational requirements during data transmission that make it too expensive for cost-effective embedded implementation today. If equalization should take at most 5% of the processor time and 17-tap subchannel equalizers are used, a TEQFB becomes feasible for single-core processors running at 240 MHz (multiple core processors can do with a lower speed due to the possibility of a highly parallelized TEQFB implementation).

## V. MORE THAN ONE RAYLEIGH QUOTIENT

Although the most popular design methods to find a single TEQ are based on solving a generalized eigenvalue problem (see Section III), they are in general not optimal in the sense of bit rate maximization. Several attempts have been made to design a TEQ that maximizes bit rate. As in Section IV, the bit rate is again the underlying objective function, but in this section we are focusing on *single* TEQ design. These designs vary in nature, but they can all be described in a common way as a maximization of a product of multiple Rayleigh quotients, and hence lead to a non-linear optimization problem [6]. In this section, each method is briefly reviewed, some non-linear optimization procedures are presented, and complexity is tabulated.

### A. *Maximum geometric signal-to-noise ratio (MGSNR) method*

The geometric SNR for a DMT system [37], [46], [47], [48] is defined as

$$\mathrm{SNR}_{geom} = \left(\prod_{i \in \mathcal{S}} \mathrm{SNR}_i\right)^{\frac{1}{N_u}}, \tag{29}$$

where $\mathcal{S}$ is the set of tones that carry data and $N_u$ is the number of tones in that set. For a high SNR and a fixed transmission bandwidth, maximizing the achievable bit rate is equivalent to maximizing the geometric SNR in (29) [37], [47]. After assuming equal power distribution in all subchannels and that the TEQ $\mathbf{w}$ and the TIR $\mathbf{b}$ are related through $\mathbf{R}_{yx}\mathbf{b} = \mathbf{R}_{yy}\mathbf{w}$, maximization of (29) can be rewritten as [37], [47]

$$\mathbf{b}_{\mathrm{GSNR}}^{\mathrm{opt}} = \arg\max_{\mathbf{b}} \sum_{i \in \mathcal{S}} \ln \mathbf{b}^T \mathbf{G}_i \mathbf{b} \quad \text{s.t.} \quad \mathbf{b}^T\mathbf{b} = 1 \text{ and } \mathbf{b}^T \mathbf{R}_\Delta \mathbf{b} \leq \mathrm{MSE}_{\max}, \tag{30}$$

where $\mathbf{R}_\Delta$ is given in (8), $\mathbf{G}_i$ is a matrix with DFT coefficients related to tone $i$, and the second constraint avoids equalization to a single spike.

The optimization problem in (30) is a constrained nonlinear optimization problem and does not have a closed form solution. In [37], [47], the MATLAB® optimization toolbox was used to solve (30). Recently, Laskarian and Kiaei proposed to use the gradient projection method in conjunction with projection onto convex sets as a means to find the solution of (30) [28], [49]. First, they remove the unit-norm constraint on the TIR since the origin is not a trivial solution of the problem. Then they observe that the second constraint represents a closed convex set in the $(\nu+1)$-dimensional Euclidean space: $\{\mathbf{b} \in \mathbb{R}^{\nu+1} | \mathbf{b}^T \mathbf{R}_\Delta \mathbf{b} \leq \mathrm{MSE}_{\max}\}$. Using the convexity property of the constraint set along with a suitable iterative descent method efficiently leads them to a stationary point. A feasible descent direction is obtained by taking a step along the negative gradient of the cost function followed by a projection on the constraint set. Based on [28], an outline of the algorithm and its complexity are given in Table VI.

### B. *Maximum bit rate (MBR) method*

In [26] and [50] the Maximum Bit Rate (MBR) TEQ design method was presented to maximize the bit rate *at the TEQ output*. The approximate subchannel SNR model is given by

$$\widetilde{\mathrm{SNR}}_i(\mathbf{w}) = \frac{\mathbf{w}^T \mathbf{A}_i \mathbf{w}}{\mathbf{w}^T \mathbf{B}_i \mathbf{w}}, \tag{31}$$

TABLE VI

ALGORITHM OUTLINE AND COMPLEXITY TO SOLVE (30) [28].

| Operation | Complexity (flops) |
|---|---|
| 1. Initialization: | |
| 1.1 Calculation of $\mathbf{R}_\Delta$ | $\mathcal{O}\left(L_w^2 + L_w^2\nu + L_w\nu^2\right)$ |
| 1.2 Eigenvalue decomposition of $\mathbf{R}_\Delta$ | $\mathcal{O}\left(\nu^3\right)$ |
| 2. Per iteration: | |
| 2.1 Gradient computation | $\mathcal{O}\left(N_u\nu^2\right)$ |
| 2.2 Descent update | $\mathcal{O}\left(\nu\right)$ |
| 2.3 Projection onto convex set | $\mathcal{O}\left(2\nu\right)$ |

where $\mathbf{A}_i$ and $\mathbf{B}_i$ describe the signal and noise components for tone $i$ respectively (see [26], [50] for details). The approximate bit rate is then given by

$$\tilde{b}_{\mathrm{TEQ\ OUT}}(\mathbf{w}) = f_{sym} \sum_{i \in \mathcal{S}} \log_2 \left( 1 + \frac{\widetilde{\mathrm{SNR}}_i(\mathbf{w})}{\Gamma} \right), \tag{32}$$

where $f_{sym} = 4$ kHz is the symbol rate. Arslan, Evans and Kiaei [26] propose to maximize this non-linear bit rate equation by using an advanced iterative Newton-like optimization algorithm, such as the Broyden-Fletcher-Goldfarb-Shanno quasi-Newton algorithm [51] in the MATLAB® optimization toolbox. The authors conclude that the MBR procedure is computationally expensive and not well-suited for real-time implementation on a programmable digital signal processor.

### *C. Bit rate maximizing TEQ (BM-TEQ) and maximum data rate TEQ (MDR-TEQ)*

The TEQ procedures of Sections V-A and V-B contain many approximations. Vanbleu *et al.* and Milosevic *et al.* independently suggested very similar TEQ design procedures for bit rate maximization, referred to as the bit rate maximizing TEQ (BM-TEQ) in [16] and the maximum data rate (MDR) TEQ in [52]. In both cases, the bit rate maximization problem can be written as

$$\arg\max_{\mathbf{w}} b_{\mathrm{DMT}}(\mathbf{w}) \quad = \quad \arg\min_{\mathbf{w}} \sum_{i \in \mathcal{S}} \log_2 \frac{\mathbf{w}^T \mathbf{B}_i \mathbf{w}}{\mathbf{w}^T \mathbf{A}_i \mathbf{w}}, \tag{33}$$

where $\mathbf{A}_i$ and $\mathbf{B}_i$ are tone dependent matrices (see [7], [16] for details). In [16], the bit rate is maximized *at the FEQ output* while the authors of [7] have chosen to maximize a slightly differently defined bit rate *at the FFT output* (or FEQ input).

Minimizing (33) is an unconstrained nonlinear optimization problem. When channel knowledge and noise statistics are available, standard non-linear iterative optimization algorithms, such as iterative (quasi-)Newton algorithms and simplex algorithms, can be applied to solve (33). Milosevic *et al.* [7] use the Almogy and Levin iteration [53] to find a root of the gradient of (33) that corresponds to the closest *local* maximum to the initial point. The initial point for $\mathbf{w}$ can be the TEQFB subchannel equalizer that results in the highest value of (33) for all subchannels of interest.

In [16], the authors observed (without proof) that, although the BM-TEQ cost function is often multimodal, the different local minima yield nearly optimal performance. Therefore, a *recursive* TEQ update based on a Gauss-Newton-like search direction was proposed to solve (33),

$$\mathbf{w}^k = \mathbf{w}^{k-1} - (\mathbf{H}^k(\mathbf{w}^{k-1}))^\dagger \ \mathbf{g}^k(\mathbf{w}^{k-1}), \tag{34}$$

where $\mathbf{g}^k(\mathbf{w}^{k-1})$ is the gradient of the cost function, $(\cdot)^\dagger$ is the pseudo-inverse, and $\mathbf{H}^k(\mathbf{w}^{k-1})$ is a positive semidefinite approximation of the Hessian of the cost function. The algorithm is recursive (or adaptive) since the TEQ update is based on continuously incoming data and not on noise statistics nor channel knowledge. The gradient and Hessian in (34) are obtained by [54]

- recursively estimating the Cholesky factor of $\mathcal{E}\{[Y_i^k \quad \Delta^T \mathbf{y}^k]^T[(Y_i^k)^* \quad \Delta^T\mathbf{y}^k]\}$ and the crosscorrelations $\mathcal{E}\{\Delta\mathbf{y}^k(X_i^k)^*\}$, $\mathcal{E}\{Y_i^k(X_i^k)^*\}$ for $\forall i \in \mathcal{S}$, where $Y_i^k$ is the DFT output of the received signal for tone $i$, $\Delta\mathbf{y}^k$ are $L_w$ difference terms of the received time-domain signal, and $X_i^k$ is the transmitted frequency domain symbol for tone $i$,
- evaluating the expressions for $\mathbf{H}^k$ and $\mathbf{g}^k$ as functions of $\mathbf{w}^{k-1}$.

Based on [54], an outline of the algorithm and its complexity are given in Table VII. The algorithm converges very fast (fewer than 100 iterations) and allows for further adaptation and tracking during data transmission.

## VI. Communications performance evaluation

This section presents a performance comparison of the optimal designs presented in Part I [6] and the low-complexity implementations presented in this paper. Section VI-A describes the communications performance measure, Section VI-B describes the synthetic data and results, and Section VI-C describes the measured channels and the performance of the various designs for these channels.

TABLE VII

ALGORITHM OUTLINE AND COMPLEXITY TO SOLVE (33) [54].

| Operation | Complexity (flops/iteration) |
|---|---|
| 1. Statistics update | $\mathcal{O}\left(L_w^2 + 2N_u L_w\right)$ |
| 2. Gradient and Hessian computation | $\mathcal{O}\left(2N_u L_w^2 + N_u L_w\right)$ |
| 3. Pseudo-inverse calculation of Hessian | $\mathcal{O}\left(L_w^3\right)$ |
| 4. TEQ update | $\mathcal{O}\left(L_w^2\right)$ |

### A. Communications performance measure

The performance metric adopted in this paper is the achievable bit rate for a fixed probability of error ($10^{-7}$). Bit allocation on subcarrier $i$ is calculated by

$$b_i = \log_2\left(1 + \frac{\text{SNR}_i}{\Gamma_{sim}}\right) \tag{35}$$

where $\text{SNR}_i$ is the SNR at the $i$th subcarrier, measured by averaging the output signal to noise (and residual interference) ratio at the FEQ output, and

$$\Gamma_{sim} \text{ (in dB)} = \Gamma_{gap} + \text{system margin} - \text{coding gain}. \tag{36}$$

Here, the "SNR gap" $\Gamma_{gap} = 9.8$ dB corresponds to $10^{-7}$ bit error rate, the system margin is $6$ dB, and the coding gain is $5$ dB [55]. Note that (35) is not in dB, whereas (36) is. The achievable bit rate is then $R = f_{sym} \sum_i b_i$, where $f_{sym} = 4$ kHz is the symbol rate and $\sum_i b_i$ is the number of bits per DMT symbol.

### B. Synthetic data simulations

*1) Test transmission lines:* The physical media for ADSL channels are metallic twisted pairs of wires, i.e. telephone lines. In practice, it is common to encounter transmission lines in which several segments of wire, each of different gauge and length, are connected together to form the subscriber loop. The common gauges are 0.32 mm, 0.4 mm ($26$ gauge), 0.5 mm ($24$ gauge), and 0.63 mm. The gauge changes introduce an impedance mismatch and cause signal reflections in the lines. Most lines also contain *bridged taps*, open-circuited wire pairs bridged onto the main cable pair. Bridged taps are intended to offer flexibility for future alterations in transmission lines, at the cost of significant reflections of signals.

This paper uses a group of eight loops widely used in research simulations, called the carrier serving area (CSA) loops, which were proposed by Bell Systems in the early 1970s. The impulse responses of these test loops can be obtained by using the *LINEMOD* software [56], which was developed based on two-port network transmission line theory [1, Sec. 3.5]. The simulations use the 8 CSA loops (available in [57]) in series with a $5^{th}$ order Chebyshev Type I high-pass filter with cut-on frequency at $4.8$ KHz and a high-pass filter with cut-on at $138$ kHz, which serve to filter out the "plain old telephone system" (POTS) voiceband signal and to filter out the upstream signals, respectively.

*2) Noise enviroment:* Sources of DSL noise can be classified into three categories: impulse noise, background noise, and crosstalk. Impulse noise consists of impulses occurring at random times, and background noise is usually modelled as additive white Gaussian noise (AWGN). Crosstalk arises due to the fact that twisted pairs of wires are usually bundled together in large cables, and signals can leak through from one cable to the next. A typical configuration towards the customer ("downstream") is fifty pairs with a larger gauge in one cable. In contrast, the configuration towards the central office ("upstream") often contains a much larger number of pairs of small gauge. Crosstalk is further divided into near-end crosstalk (NEXT) and far-end crosstalk (FEXT). NEXT tends to be dominant in ADSL transmissions [1]. It is generally modelled as a coupling filter fed by a white signal that has the same bandwidth and statistical properties as the modulated signal used by the adjacent loops. Our simulations use NEXT corresponding to 5 ISDN disturbers plus AWGN at -140 dBm/Hz, distributed over the entire bandwidth (relative to 23 dBm input signal power).

*3) Simulation results:* The FFT size is $N = 512$ and the CP length is $\nu = 32$, as in the G.DMT standard for downstream transmission. Delay optimization has been applied to all methods. The TEQ length is 17 taps, which is a common choice in practice. Fig. 1 compares designs that are optimal in terms of some cost function other than the bit rate, Fig. 2 presents the results for sub-optimum methods that make approximations or use a limited number of iterations (1000 iterations in this case), Fig. 3 presents the results for methods that explicitly attempt to maximize the bit rate, and Fig. 4 presents the bit rate vs. delay for various TEQ designs, using CSA loop 4.

The dual path TEQ computed the MMSE, MSSNR, and MDS TEQs, and picked the best one for one path, then designed a Min-ISI TEQ optimized over a subset of tones for the second path.

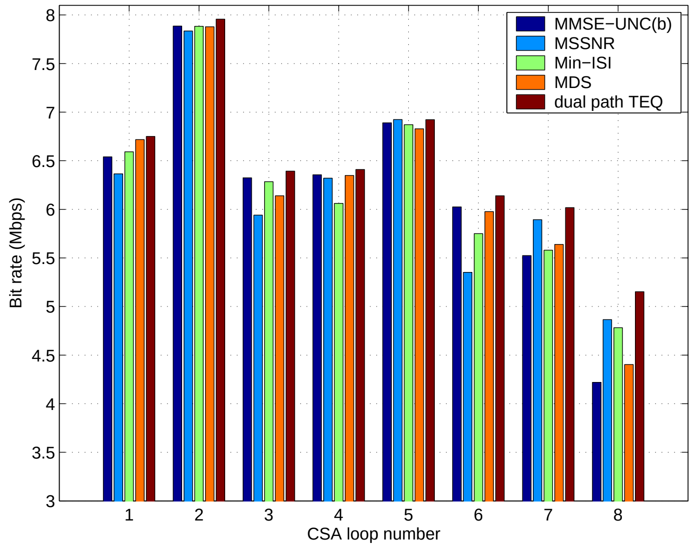


Fig. 1. Bit rate of designs that are optimal in terms of a measure other than the bit rate: minimum mean squared error (MMSE), maximum shortening SNR (MSSNR), minimum intersybol interference (Min-ISI), minimum delay spread (MDS), and dual path TEQ. Left-to-right corresponds to top-to-bottom on the legend.

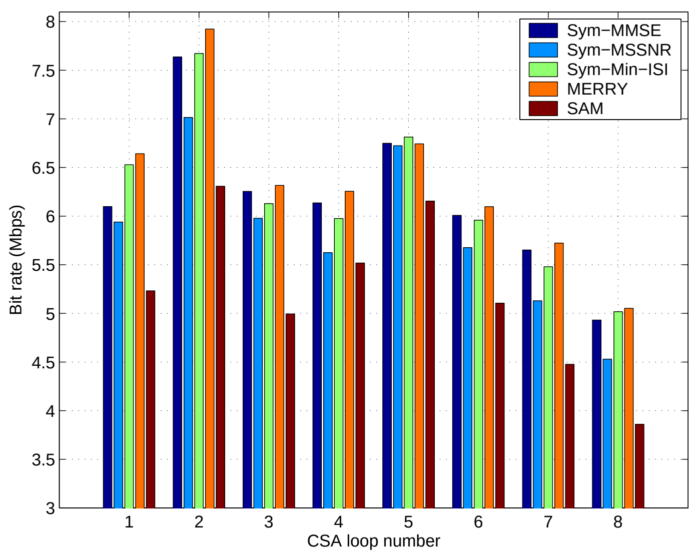


Fig. 2. Bit rate of designs that make approximations or use a limited number of iterations: symmetric minimum mean squared error (Sym-MMSE), symmetric maximum shortening SNR (Sym-MSSNR), symmetric minimum intersybol interference (Sym-Min-ISI), multicarrier equalization by restoration of reduncancy (MERRY), and sum-squared auto-correlation minimization (SAM). Left-to-right corresponds to top-to-bottom on the legend.

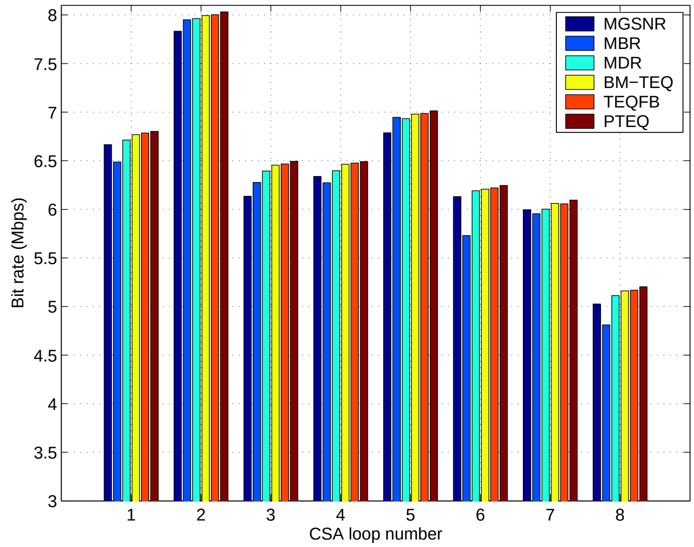


Fig. 3. Bit rate of TEQ designs that explicitly attempt to maximize the bit rate: maximum geometric SNR (MGSNR), maximum bit rate (MBR), maximum data rate (MDR), bitrate maximizing TEQ (BM-TEQ), TEQ filter bank (TEQFB), and per-tone equalization (PTEQ). Left-to-right corresponds to top-to-bottom on the legend.

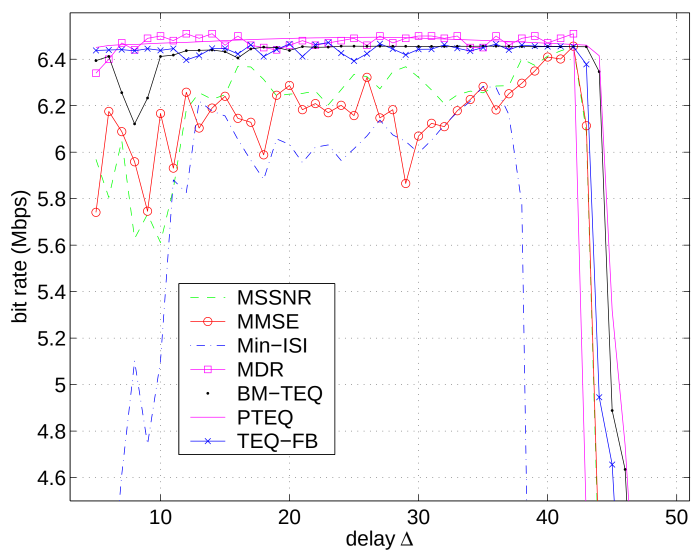


Fig. 4. Bit rate versus delay for various TEQ designs, using CSA loop 4.

As such, it outperforms the other designs in Fig. 1. The approximations used in Fig. 2 usually induce a small loss in bit rate with respect to their counterparts in Fig. 1. The SAM algorithm seems to become stuck in false local (but not global) minima of the SAM cost function, leading to a performance loss. The algorithms in Fig. 3 are listed in order of fewer approximations and more general structures; hence performance is expected to (and generally does) increase as we move left to right on the bar chart. From Fig. 4, the MDR, BM-TEQ, TEQFB, and PTEQ do not require a full delay search in order to achieve good performance, whereas most of the other designs are sensitive to the choice of delay and thus require a thorough delay search to achieve optimal performance.

### *C. AST data set*

Applied Signal Technology has generously provided the authors with several measured ADSL data signals. The voltage signal from a telephone line was recorded, sampled at 2.5 MHz, and digitized. The signal was frequency-duplexed so that the upstream and downstream channels lay in two distinct frequency bands [1].

We resampled the data to exactly 2.208 MHz, and then used the C-REVERB2 training sequence to perform a (downstream) channel estimate. The estimated channel is given by

$$\hat{\mathbf{h}} = \mathcal{F}_N{}^{-1} \left( \frac{1}{1000} \sum_{k=1}^{1000} \frac{\mathcal{F}_N \mathbf{x}^k}{\mathcal{F}_N \mathbf{y}^k} \right), \tag{37}$$

where vector division is performed pointwise. Here, $\mathcal{F}_N$ is the DFT matrix, $\mathbf{x}^k$ is the $k^{th}$ period of the chosen C-REVERB2 signal, and $\mathbf{y}^k$ is the corresponding received signal over the same period. The C-REVERB2 signal is generated according to the definition in [58, Sec. 10.4.5]. Fig. 5 shows the impulse responses of the estimated channels for two sets of recorded data, including the POTS splitters.

Fig. 6 shows the achievable bit rate for the 16 TEQ designs considered in the previous simulations, except now they have been used to equalize the two AST channels from Fig. 5. These results corroborate the results from the synthetic channels in Figs. 1–3.

## VII. CONCLUSION

Equalizer design for multicarrier systems can be a computationally intensive procedure. We have surveyed the TEQ design literature for complexity reduction techniques, and tabulated the complexity requirements of the most popular algorithms. We have also provided a performance assessment in the form of bit rate computation for designs using both synthetic and measured DSL channels. For ADSL channels, most designs yield bit rates that only differ by about 10%,

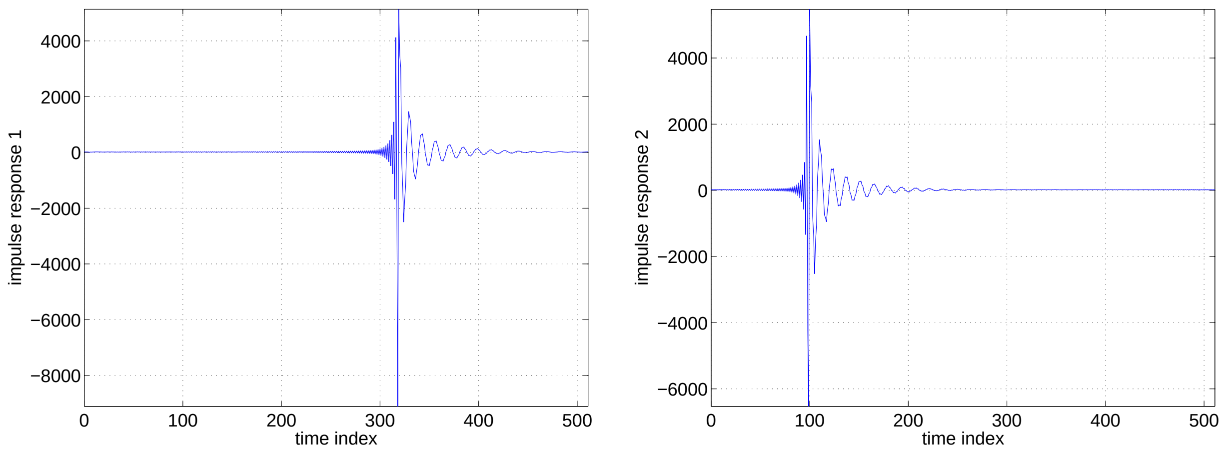


Fig. 5. Estimated channel impulse responses for measured signals 1 and 2 from the Applied Signal Technology data set.

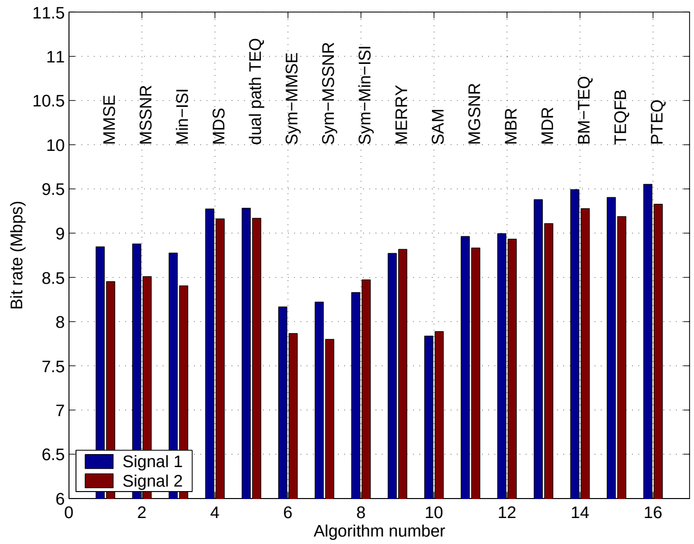


Fig. 6. Bit rate acheived using the two measured AST channels. The channel impulse responses are given in Fig. 5.

but computational requirements can vary by several orders of magnitude. The literature appears to be moving towards more costly implementations with the goal of ever-increasing bit rates.

## ACKNOWLEDGEMENTS

The authors wish to thank Applied Signal Technology (Sunnyvale, CA) for providing the measured ADSL data, and Mike Woodhall (formerly at Applied Signal Technology) for answering our many questions about the manner in which this ADSL data was measured.

# REFERENCES


[1] T. Starr, J.M. Cioffi, and P.J. Silvermann, *Understanding Digital Subscriber Line Technology*, Prentice Hall PTR, Upper Saddle River, NJ, 1999.

[2] The Inst. of Electrical and Electronics Engineers, "Wireless LAN Medium Access Control (MAC) and Physical Layer (PHY) Specifications. IEEE Std. 802.11a," 1999 Edition.

[3] The European Telecomm. Standards Inst., "Broadband Radio Access Networks (BRAN); High Performance Radio Local Area Networks (HIPERLAN) Type 2; System Overview," ETR101 683 114, 1999.

[4] The European Telecomm. Standards Inst., "Digital Video Broadcasting (DVB); Framing Structure, Channel Coding and Modulation for Digital Terrestrial Television," ETSI EN 300 744 V1.4.1, 2001 Edition.

[5] The European Telecomm. Standards Inst., "Radio Broadcasting System, Digital Audio Broadcasting (DAB) to Mobile, Portible, and Fixed Receivers," ETS 300 401, 1995–1997.

[6] R. K. Martin, K. Vanbleu, M. Ding, G. Ysebaert, M. Milosevic, B. L. Evans, M. Moonen, and C. R. Johnson, Jr., "Multicarrier Equalization: Unification and Evaluation. Part I: Optimal Designs," Submitted to *IEEE Transactions on Signal Processing*, Dec. 2003.

[7] M. Milosevic, L. F. C. Pessoa, B. L. Evans, and R. Baldick, "DMT Bit Rate Maximization with Optimal Time Domain Equalizer Filter Bank Architecture," in *Proc. IEEE Asilomar Conf.*, Pacific Grove, CA, Nov. 2002, vol. 1, pp. 377–382.

[8] K. Van Acker, G. Leus, M. Moonen, O. van de Wiel, and T. Pollet, "Per Tone Equalization for DMT-Based Systems," *IEEE Trans. on Comm.*, vol. 49, no. 1, pp. 109–119, Jan. 2001.

[9] N. Al-Dhahir and J. M. Cioffi, "Efficiently Computed Reduced-Parameter Input-Aided MMSE Equalizers for ML Detection: A Unified Approach," *IEEE Trans. on Info. Theory*, vol. 42, no. 3, pp. 903–915, May 1996.

[10] G. H. Golub and C. F. Van Loan, *Matrix Computations*, The Johns Hopkins University Press, Baltimore, MD, 1996.

[11] J. Wu, G. Arslan, and B. L. Evans, "Efficient Matrix Multiplication Methods to Implement a Near-Optimum Channel Shortening Method for Discrete Multitone Transceivers," in *Proc. IEEE Asilomar Conf. on Signals, Systems, and Computers*, Pacific Grove, CA, Nov. 2000, vol. 1, pp. 152–157.

[12] R. K. Martin, M. Ding, B. L. Evans, and C. R. Johnson, Jr., "Efficient Channel Shortening Equalizer Design," to appear in *EURASIP Journal on Applied Signal Processing, second quarter, 2004.*

[13] R. Schur and J. Speidel, "An Efficient Equalization Method to Minimize Delay Spread in OFDM/DMT Systems," in *Proc. IEEE Int. Conf. on Comm.*, Helsinki, Finland, June 2001, vol. 5, pp. 1481–1485.

[14] A. Tkacenko and P. P. Vaidyanathan, "Noise Optimized Eigenfilter Design of Time-domain Equalizers for DMT Systems," in *Proc. IEEE Int. Conf. on Comm.*, New York, NY, Apr.–May 2002, vol. 1.

[15] A. Tkacenko and P. P. Vaidyanathan, "A Low-Complexity Eigenfilter Design Method for Channel Shortening Equalizers for DMT Systems," *IEEE Trans. on Comm.*, vol. 51, no. 7, July 2003.

[16] K. Vanbleu, G. Ysebaert, G. Cuypers, M. Moonen, and K. Van Acker, "Bitrate Maximizing Time-Domain Equalizer Design for DMT-based Systems," to appear in *IEEE Trans. on Comm.*

[17] I. Lee, J. S. Chow, and J. M. Cioffi, "Performance Evaluation of a Fast Computation Algorithm for the DMT in High-speed Subscriber Loop," *IEEE Journal on Selected Areas in Comm.*, vol. 13, no. 9, pp. 1564–1570, Dec. 1995.

[18] N. Lashkarian and S. Kiaei, "Fast Algorithm for Finite-length MMSE Equalizers with Application to Discrete Multitone Systems," in *IEEE International Conference on Acoustics, Speech, and Signal Processing*, Mar. 1999, vol. 5, pp. 2753–2756.

[19] R. M. Gray, "Toeplitz and Circulant Matrices: A Review," [Online]. Available: http://ee.stanford.edu/∼gray/toeplitz.pdf.

[20] R. K. Martin, C. R. Johnson, Jr., M. Ding, and B. L. Evans, “Exploiting Symmetry in Channel Shortening Equalizers,” in *Proc. Int. Conf. on Acoustics, Speech, and Signal Proc.*, Hong Kong SAR, China, Apr. 2003, vol. 5, pp. V–97–V–100.

[21] R. K. Martin, C. R. Johnson, Jr., M. Ding, and B. L. Evans, “Infinite Length Results for Channel Shortening Equalizers,” in *Proc. IV IEEE Sig. Proc. Workshop on Sig. Proc. Advances in Wireless Comm.*, Rome, Italy, June 2003.

[22] C. Ribeiro, V. Silva, and P. S. R. Diniz, “Linear Phase Impulse Response Shortening for xDSL DMT Modems,” in *IEEE Int. Telecommunications Symp.*, Brasil, Sept. 2002, pp. 368–371.

[23] M. Ding, B. L. Evans, R. K. Martin, and C. R. Johnson, Jr., “Minimum Intersymbol Interference Methods for Time Domain Equalizer Design,” in *Proc. IEEE Global Comm. Conf.*, San Francisco, CA, Dec. 2003.

[24] J. S. Chow, J. C. Tu, and J. M. Cioffi, “A Discrete Multitone Transceiver System for HDSL Applications,” *IEEE Journal on Selected Areas in Comm.*, vol. 9, no. 6, pp. 895–907, Aug. 1991.

[25] M. Ding, A. J. Redfern, and B. L. Evans, “A Dual-path TEQ Structure for DMT-ADSL Systems,” in *Proc. IEEE Int. Conf. on Acoustics, Speech, and Signal Proc.*, San Francisco, CA, May 2002, vol. 3, pp. 2573–2576.

[26] G. Arslan, B. L. Evans, and S. Kiaei, “Equalization for Discrete Multitone Receivers To Maximize Bit Rate,” *IEEE Trans. on Signal Processing*, vol. 49, no. 12, pp. 3123–3135, Dec. 2001.

[27] M. Nafie and A. Gatherer, “Time-Domain Equalizer Training for ADSL,” in *Proc. IEEE Int. Conf. on Comm.*, Montreal, Canada, June 1997, vol. 2, pp. 1085–1089.

[28] N. Lashkarian and S. Kiaei, “Optimum Equalization of Multicarrier Systems: A Unified Geometric Approach,” *IEEE Trans. on Comm.*, vol. 49, pp. 1762–1769, Oct. 2001.

[29] R. K. Martin, J. Balakrishnan, W. A. Sethares, and C. R. Johnson, Jr., “A Blind, Adaptive TEQ for Multicarrier Systems,” *IEEE Signal Processing Letters*, vol. 9, no. 11, pp. 341–343, Nov. 2002.

[30] K. Van Acker, G. Leus, M. Moonen, and T. Pollet, “RLS-Based Initialization for Per-Tone Equalizers in DMT Receivers,” *IEEE Trans. on Comm.*, vol. 51, no. 6, pp. 885–889, June 2003.

[31] G. Ysebaert, K. Vanbleu, G. Cuypers, M. Moonen, and T. Pollet, “Combined RLS-LMS Initialization for Per Tone Equalizers in DMT-Receivers,” *IEEE Trans. on Signal Processing*, vol. 51, no. 7, pp. 1916–1927, July 2003.

[32] P. I. Davis, N. J. Higham, and F. Tisseur, “Analysis of the Cholesky Method With Iterative Refinement For Solving the Symmetric Definite Generalized Eigenproblem,” *SIAM Journal Matrix Anal. Appl.*, vol. 23, no. 2, pp. 472–493, 2001.

[33] S. Celebi, “Interblock Interference (IBI) Minimizing Time-Domain Equalizer (TEQ) for OFDM,” *IEEE Signal Processing Letters*, vol. 10, no. 8, pp. 232–234, Aug. 2003.

[34] C. Chatterjee, V. P. Roychowdhury, J. Ramos, and M. D. Zoltowski, “Self-Organizing Algorithms for Generalized Eigen-Decomposition,” *IEEE Trans. on Neural Networks*, vol. 8, no. 6, pp. 1518–1530, Nov. 1997.

[35] D. D. Falconer and F. R. Magee, “Adaptive Channel Memory Truncation for Maximum Likelihood Sequence Estimation,” *Bell Sys. Tech. Journal*, pp. 1541–1562, Nov. 1973.

[36] B. Farhang-Boroujeny and M. Ding, “Design Methods for Time-Domain Equalizers in DMT Transceivers,” *IEEE Trans. on Comm.*, vol. 49, no. 3, pp. 554–562, Mar. 2001.

[37] N. Al-Dhahir and J. M. Cioffi, “Optimum Finite-Length Equalization for Multicarrier Transceivers,” *IEEE Trans. on Comm.*, vol. 44, no. 1, pp. 56–64, Jan. 1996.

[38] J. S. Chow, J. M. Cioffi, and J. A. C. Bingham, “Equalizer Training Algorithms for Multicarrier Modulation Systems,” in *Proc. IEEE Int. Conf. on Comm.*, Geneva, Switzerland, May 1993, pp. 761–765.

[39] K. Van Acker, *Equalization and Echo Cancellation for DMT-based DSL Modems*, Ph.D. thesis, Katholieke Universiteit Leuven, Jan. 2001, ftp://ftp.esat.kuleuven.ac.be/pub/sista/vanacker/reports/01-02.ps.gz.

[40] P. J. W. Melsa, R. C. Younce, and C. E. Rohrs, "Impulse Response Shortening for Discrete Multitone Transceivers," *IEEE Trans. on Comm.*, vol. 44, pp. 1662–1672, Dec. 1996.

[41] C. Yin and G. Yue, "Optimal Impulse Response Shortening for Discrete Multitone Transceivers," *Electronics Letters*, vol. 34, pp. 35–36, Jan. 1998.

[42] I. Ilani, "Time Domain Equalizer for DMT Transceivers – A Geometric Approach," US patent no. 6341298, Jan. 2002.

[43] M. de Courville, P. Duhamel, P. Madec, and J. Palicot, "Blind equalization of OFDM systems based on the minimization of a quadratic criterion," in *Proc. IEEE Int. Conf. on Comm.*, Dallas, TX, June 1996, pp. 1318–1321.

[44] F. Romano and S. Barbarossa, "Non-Data Aided Adaptive Channel Shortening for Efficient Multi-Carrier Systems," in *Proc. IEEE Int. Conf. on Acoustics, Speech and Signal Proc.*, Hong Kong SAR, China, Apr. 2003, vol. 4, pp. 233–236.

[45] M. Milosevic, *Maximizing Data Rate of Discrete Multitone Systems using Time Domain Equalization Design*, Ph.D. thesis, The University of Texas at Austin, May 2003.

[46] N. Al-Dhahir and J. Cioffi, "A Band-optimized Reduced-complexity Equalized Multicarier Transceiver," *IEEE Trans. on Comm.*, vol. 45, pp. 948–956, Aug. 1997.

[47] N. Al-Dhahir and J. M. Cioffi, "Optimum Finite-Length Equalization for Multicarrier Transceivers," in *Proc. IEEE Global Comm. Conf.*, San Francisco, CA, Nov. 1994, pp. 1884–1888.

[48] N. Al-Dhahir and J. Cioffi, "The Combination of Finite-length Geometric Equalization and Candwidth Optimization for Multicarrier Transceivers," in *International Conf. on Acoustics, Speech, and Signal Processing*, May 1995, pp. 1201–1204.

[49] N. Lashkarian and S. Kiaei, "Optimum Equalization of Multicarrier Systems Via Projection Onto Convex Set," in *IEEE Int. Conf. on Comm.*, Vancouver, June 1999, vol. 2, pp. 968–972.

[50] G. Arslan, *Equalization Techniques for Multicarrier Modulation*, Ph.D. thesis, The Univ. of Texas at Austin, Dec. 2000.

[51] W. H. Press, S. A. Teukolsky, W. T. Vetterling, and B. P. Flannery, *Numerical Recepies in C*, Cambridge University Press, New York, NY, 2 edition, 1992.

[52] M. Milosevic, L. F. C. Pessoa, and B. L. Evans, "Simultaneous Multichannel Time Domain Equalizer Design Based On The Maximum Composite Shortening SNR," in *Proc. IEEE Asilomar Conf.*, Pacific Grove, CA, Nov. 2002, vol. 2, pp. 1895–1899.

[53] Y. Almogy and O. Levin, "A Class of Fractional Programming Problems," *Operations Research*, vol. 19, pp. 57–67, 1971.

[54] K. Vanbleu, G. Ysebaert, G. Cuypers, and M. Moonen, "Bitrate Maximizing Per-Group Equalization for DMT-based Systems," Submitted to *Elsevier Signal Processing*.

[55] J. M. Cioffi, "A Multicarrier Primer," [Online]. Available: http://www-isl.stanford.edu/people/cioffi/pdf/multicarrier.pdf.

[56] D. G. Messerschmitt and A. Salvekar, "Linemod software for transmission line analysis," Stanford University. [Online]. Available: http://www.stanford.edu/∼cioffi/linemod/linemod.html.

[57] G. Arslan, M. Ding, B. Lu, M. Milosevic, Z. Shen, and B. L. Evans, "MATLAB DMTTEQ Toolbox 3.1 Beta 3 Release," The University of Texas at Austin, July 27, 2003. [Online.] Available: http://www.ece.utexas.edu/∼bevans/projects/adsl/dmtteq/dmtteq.html.

[58] International Telecommunications Union, "Asymmetrical Digital Subscriber Line (ADSL) Transceivers," ITU, 1999.

[59] W. Henkel and T. Kessler, "Maximizing the Channel Capacity of Multicarrier Transmission by Suitable Adaptation of the Time-domain Equalizer," *IEEE Trans. on Comm.*, vol. 48, no. 12, pp. 2000–2004, Dec. 2000.

[60] W. Kozek, "A Subspace Method for TEQ-Adaptation in FFT-based Multicarrier Receivers," in *Proceedings of the 5th International OFDM-Workshop*, Hamburg, Germany, Sept. 2000, pp. 39.1–39.4.